

# Modelling optical fiber for LPGFS systems

LAURENTIU BASCHIR<sup>1</sup>, DAN SAVASTRU, SORIN MICLOS\*

National Institute of R&D for Optoelectronics - INOE 2000, 409 Atomistilor St., Magurele, Ilfov, RO-077125, Romania

A reliable and consistent model of the optical fiber intended to be used in Long Period Grating Fiber Sensors design is proposed. The model uses mechanical and optical parameters either specified by the manufacturer or calculated from specified parameters. Two different approaches were used, as some parameters or others are known. The method was tested on optical fibers of two major manufacturers, the resulting models being in a good concordance with given specifications. This optical fiber modelling method provides a very useful and powerful tool for Long Period Grating Fiber Sensors designers.

(Received May 27, 2021; accepted October 7, 2021)

**Keywords:** Optical fiber model, LPGFS design, Fiber grating optical sensors

## 1. Introduction

Optical fiber based refractometric sensing devices represents a very attractive solution for measurement of a wide range of parameters: mechanical (stress [1], torsion [2,3], temperature [4], vibration [5], structural health [6,7]), chemical (concentrations [8], diffusion [9]), biological (presence of pathogenic bacteria [10,11]). A SPR (Surface Plasmonic Resonance) approach for sensors was proposed by several authors [12-16]. Another approaches using optical fiber sensors are described in [17].

Among these sensor types LPGFS (Long Period Grating Fiber Sensors) represents a promising technology, with many benefits: high sensitivity, immunity to electromagnetic interferences, chemically and biologically inert, small size, and capability for in-situ, real-time, remote, and distributed sensing. The design of such LPGFS sensors requires a proper modeling of light guided propagation through optical fiber core and choosing the proper pitch of the grating [18-25].

The design is based on knowing some parameters of the optical fiber. Some of them are specified by the manufacturer, while other can be calculated from the specified ones. Not all needed parameters are directly specified, therefore they have to be “retrieved” using other parameters or information. The aim of this research is to set up a reliable and consistent model of the optical fiber that we intend to use in LPGFS design.

## 2. Theory

### 2.1. Optical fiber parameters used in LPG design

There are some parameters needed when designing a LPG. First are needed geometrical parameters: core radius,  $a_{co}$  and cladding radius  $a_{cl}$ . Then are needed some optical parameters: the refractive index of core  $n_{co}$  and the refractive of cladding  $n_{cl}$  over the operating wavelength  $\lambda$  range. Some parameters can be deduced from the

parameters mentioned above: numerical aperture  $NA$ , refractive index difference  $\Delta$ , V-number or the normalized frequency  $V$ , mode field diameter  $MFD$ . The next equations express their relationships:

$$NA = \sqrt{n_{co}^2 - n_{cl}^2} \quad (1)$$

$$\Delta = \frac{n_{co}^2 - n_{cl}^2}{2 \cdot n_{co}^2} \quad (2)$$

$$V = 2 \cdot a_{co} \cdot \pi \cdot NA / \lambda \quad (3)$$

Mode field diameter is calculated using Marcuse equation [26] as:

$$MFD = 2 \cdot a_{co} \cdot (0.65 + 1.619 \cdot V^{-1.5} + 2.879 \cdot V^{-6}) \quad (4)$$

A relative MFD may be obtained by dividing MFD to the core diameter:

$$MFD_{rel} = 0.65 + 1.619 \cdot V^{-1.5} + 2.879 \cdot V^{-6} \quad (5)$$

This function depends only on V, as shown in Fig. 1. From Eq. (5) and Eq. (3) it results that higher values of  $MFD_{rel}$  correspond to lower values of V and higher values of  $\lambda$ . Conversely, lower values of  $MFD_{rel}$  correspond to higher values of V and lower values of  $\lambda$ . Practically,  $MFD_{rel}$  should be larger than 1 ( $MFD$  is always greater than core diameter) and is usually less than 1.33.

Some manufacturers provide information about  $a_{co}$ ,  $NA$  and  $MFD$  but don't specify  $n_{co}$  and  $n_{cl}$ , while others provide information about  $NA$ ,  $MFD$ ,  $n_{co}$  and  $n_{cl}$  but don't specify  $a_{co}$ . Therefore two different approaches should be considered, whether  $a_{co}$  is specified or not. In the first approach from Eq. (4) a value for V is found corresponding to the specified  $MFD$ . Then NA is calculated reversing Eq. (3). A special attention should be paid to the fact that the numerical aperture specified by the manufacturer is sometimes that measured in far field at the 1% power level, instead of  $1/e^2$  as presumed in LPG design theory.

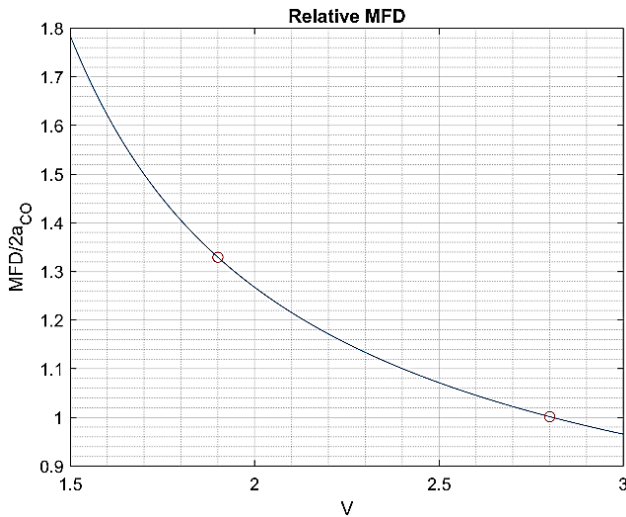


Fig. 1. Relative MFD. Typical limits for  $V$  (1.9 and 2.8) are shown in red circles (color online)

In the second approach knowing  $MFD$  and  $NA$  and combining Eq. (3) and Eq. (4) the appropriate  $V$  is calculated. From Eq. (3) it results  $a_{co}$ .

In the first approach usually  $MFD$  is specified by the manufacturer for two wavelengths  $\lambda$ . A first guess is done by finding the values of  $V$  that satisfy Eq. (4) for specified values of  $MFD$ . The reversal of Marcuse equation to obtain the  $V$  values is done by the method of halving the interval. The starting interval limits of  $V$  are 1.9 and 2.8, corresponding to  $MFD_{rel}$  values 1.33 and 1 respectively.

## 2.2. Determining core refractive index

Reversing Eq. (3) a new value is obtained for  $NA$ , which will be used to determine  $n_{co}$ , from Eq. (1). Note that  $n_{cl}$  is the refractive index of the cladding, made of fused silica ( $SiO_2$ ), while  $n_{co}$  is the refractive index of the core, made of fused silica doped with  $GeO_2$ . The doping concentration  $d_{Ge}$  is considered when calculating  $n_{co}$ . The dispersion equation of the refractive index of  $SiO_2$ ,  $GeO_2$  and of the doped glass is given by Sellmeier formula:

$$n(\lambda) = \sqrt{1 + \sum_1^3 \frac{A_i \cdot \lambda^2}{\lambda^2 - B_i^2}} \quad (6)$$

where  $A_i$  and  $B_i$  are coefficients specified in [27] for  $SiO_2$  and  $GeO_2$ . Sellmeier equation can be written for  $n_{cl}$ ,  $n_G$  (the refractive index of  $GeO_2$ ) and  $n_{co}$ :

$$n_{cl} = \sqrt{1 + \sum_1^3 \frac{A_{cli} \cdot \lambda^2}{\lambda^2 - B_{cli}^2}} \quad (7)$$

$$n_G = \sqrt{1 + \sum_1^3 \frac{A_{Gi} \cdot \lambda^2}{\lambda^2 - B_{Gi}^2}} \quad (8)$$

$$n_{co} = \sqrt{1 + \sum_1^3 \frac{A_{coi} \cdot \lambda^2}{\lambda^2 - B_{coi}^2}} \quad (9)$$

Regarding the refractive index of core, considering a doping concentration  $d_{Ge}$  of  $GeO_2$ , the coefficients  $A_{coi}$  and  $B_{coi}$  are calculated as it follows [28]:

$$A_{coi} = A_{cli} + d_{Ge} \cdot (A_{Gei} - A_{cli}) \quad (10)$$

$$B_{coi} = B_{cli} + d_{Ge} \cdot (B_{Gei} - B_{cli}) \quad (11)$$

From Eq. (9) to (11) the value of  $d_{Ge}$  is calculated to get the required  $n_{co}$  that satisfies Eq. (1).

## 3. Results

For the first approach we studied Corning SMF28e+® Photonic fiber, while for the second approach we studied five FiberCore fibers: SM980 (4.5/125), SM980 (5.8/125), SM1250 (9/80), SM1500 (9/125) and SM1500ES (3/125). Their specifications are summarized in Table 1.

Table 1. Optical fibers specifications

Parameter	SMF 28e+	SM 980 (4.5/125)	SM 980 (5.8/125)	SM 1250 (9/80)	SM 1500 (9/125)	SM 1500ES (3/125)
$\lambda$ , nm	1280 – 1650	980 – 1550	980 – 1550	1310 – 1550	1520 – 1650	1510 – 1650
$\lambda_{cut}$ , nm	$\leq 1280$	870 – 970	870 – 970	1150 – 1250	1300 – 1500	1400 – 1500
$\lambda_{op}$ , nm	1310 1550	980	980	1310	1550	1550
$MFD$ , $\mu m$	9.2 10.4	4.5	5.8	9	9	3.2
$2a_{co}$ , $\mu m$	8.2	-	-	-	-	-
$NA$	0.14*	0.18	0.14	0.12	0.14	0.40
Type	I	II	II	II	II	II

\* The manufacturer specified a value measured at 1% power level, not at  $1/e^2$ , so this value wasn't considered as specification.

### 3.1. First approach procedure

For the approach of type I the core diameter ( $2a_{co} = 8.2 \mu m$ ) is specified and also  $MFD$  (9.2 and  $10.4 \mu m$ ) for two operating wavelengths (1310 and 1550 nm).

From Eq. (4) it results two values for  $V$ : 2.3337 for 1310 nm and 1.9984 for 1550 nm. Corresponding  $NA$  values are: 0.1187 and 0.1202 respectively. From Eq. (9) to (11) the value of  $d_{Ge}$  is calculated to get the required  $n_{co}$  that satisfies Eq. (1): 3.2525 %, respectively 3.3271 %.

But  $d_{Ge}$  is unique over the whole wavelength range so tolerances were given to  $MFD$ : 9.15 to 9.25  $\mu m$ , rounded 9.2  $\mu m$  and 10.35 to 10.45  $\mu m$ , rounded 10.4  $\mu m$ . Values of  $d_{Ge}$  are calculated again for these new  $MFD$  values.

Table 2. Doping concentration for different MFD

$\lambda_{op}$ , nm	1310 nm			1550 nm		
$MFD$ , $\mu m$	9.25	9.20	9.15	10.45	10.40	10.35
$V$	2.3159	2.3337	2.3520	1.9877	1.9984	2.0093
$d_{Ge}$ , %	3.2030	3.2525	<b>3.3036</b>	<b>3.2917</b>	3.3271	3.3634

The doping concentration  $d_{Ge}$  variation within  $MFD$  tolerances is presented in Fig. 2. It can be seen that doping concentration can be the same for both wavelength only when it takes values between 3.2917 % and 3.3036 %. A reasonable supposition is that the unique value of  $d_{Ge}$  is prescribed (as nominal value) with a 2-significant digits precision. Thus we set this value to 3.3 %.

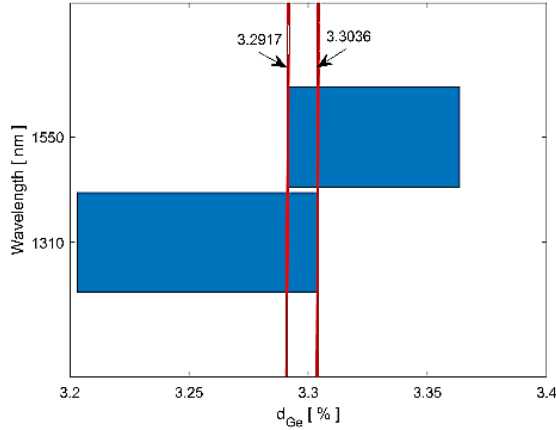


Fig. 2. Doping concentration  $d_{Ge}$  for  $MFD$  variation range, at two wavelengths (color online)

With this value  $n_{co}$  was calculated using Eqs. (9) to (11), resulting corrected values of  $NA$ ,  $V$  and  $MFD$ :

Table 3.  $NA$ ,  $V$  and  $MFD$  recalculated for  $d_{Ge} = 3.3\%$

$\lambda_{op}$ , nm	1310	1550
$NA$	0.1195	0.1197
$V$	2.3507	1.9902
$MFD$ , $\mu\text{m}$	9.1535	10.4381

Calculated  $MFD$  values can be rounded at 0.1  $\mu\text{m}$ , obtaining the specified data: 9.2 and 10.4  $\mu\text{m}$ .  $NA$  is practically 0.12 for all the wavelength range.

A plot of refractive index of core ( $n_{co}$ ), of cladding ( $n_{cl}$ ), refractive group index of core ( $n_{gco}$ ) and of cladding ( $n_{gcl}$ ) over all wavelengths range (1280-1650 nm) is shown in Fig. 3. The chromatic dispersion of the refractive indices of the two materials (core and cladding) is important and should be taken into account when designing a LPGFS.

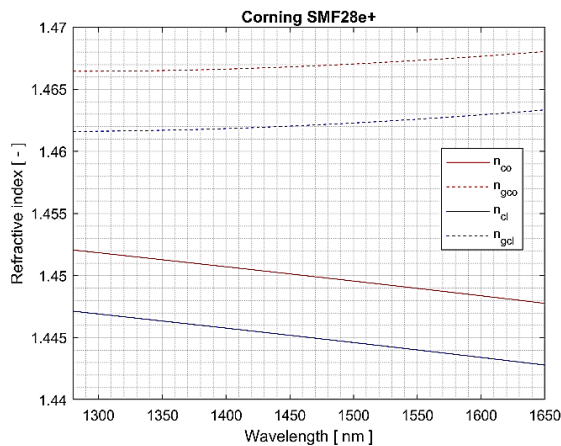


Fig. 3. Refractive index of core, cladding, group index of core and cladding (color online)

$V$  is calculated using Eq. (3), as it can be seen in Fig. 4. Maximum  $V$  is about 2.4 and is obtained at  $\lambda = 1280$  nm, that is the cut-off wavelength  $\lambda_c$  was reached.

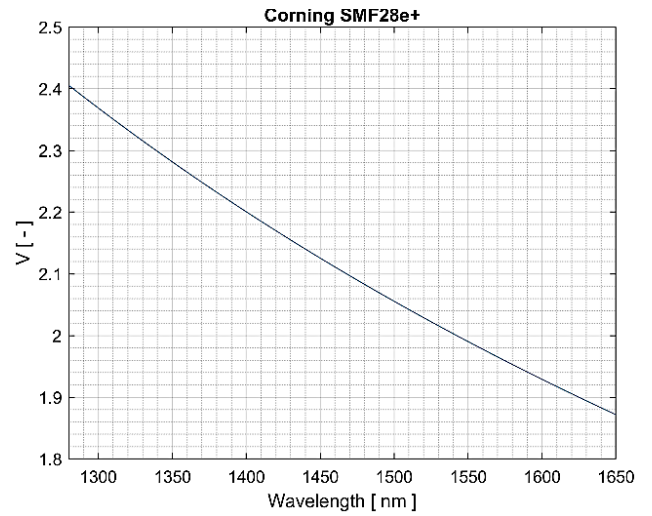


Fig. 4.  $V$  dependence on wavelength (color online)

In Fig. 5 is presented the dependence of  $MFD$  on the wavelength.

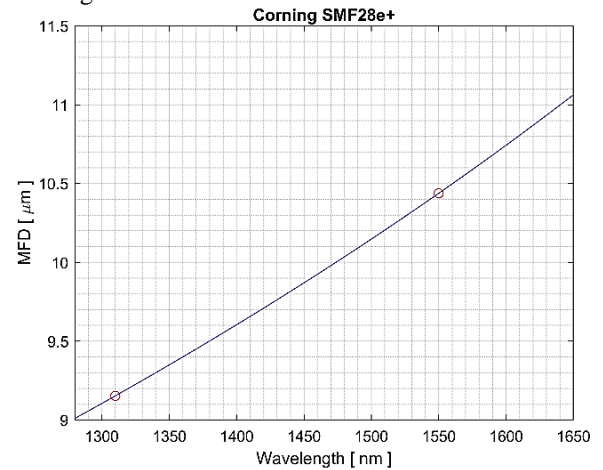


Fig. 5.  $MFD$  vs. wavelength. The red circles mark the specification wavelengths (1310 and 1550 nm) (color online)

### 3.2. Second approach procedure

Five optical fibers, manufactured by FiberCore (SM980 (4.5/125), SM980 (5.8/125), SM1250 (9/80), SM1500 (9/125) and SM1500ES (3/125)), were studied using the second approach. For each fiber only  $NA$  and  $MFD$  were specified for one operating wavelength  $\lambda_{op}$  (see Table 1).

The procedure begins with the calculation of  $n_{co}$  from Eq. (1) and of  $d_{Ge}$  from Eq. (9) to (11). As in the first approach, these values were rounded up to two significant digits ( $d_{Ger}$ ).  $NA$  were recalculated using  $d_{Ger}$  (getting  $NA_r$ ). All these data are summarized in Table 4.

Table 4. NA and  $d_{Ge}$ 

Parameter	SM 980 (4.5/125)	SM 980 (5.8/125)	SM 1250 (9/80)	SM 1500 (9/125)	SM 1500ES (3/125)
$\lambda_{op}$ , nm	980	980	1310	1550	1550
NA	0.18	0.14	0.12	0.14	0.40
$d_{Ge}$ , %	7.4669	4.5178	3.3256	4.5107	36.8603
$d_{Ger}$ , %	7.5	4.5	3.3	4.5	36.9
$NA_r$	0.1804	0.1397	0.1195	0.1398	0.4002

Next step is to calculate  $V$  using Eq. (3) and (4), eliminating  $a_{co}$ . Then  $2a_{co}$  was determined from Eq. (4) and rounded at 0.1  $\mu\text{m}$ , resulting  $2a_{cor}$ . Using this value  $V$  and  $MFD$  were recalculated (from Eq. (3), respectively Eq. (4)), obtaining  $V_r$  and  $MFD_r$ . Table 5 summarizes these results.

Table 5.  $V$ ,  $a_{co}$  and  $MFD$ 

Parameter	SM 980 (4.5/125)	SM 980 (5.8/125)	SM 1250 (9/80)	SM 1500 (9/125)	SM 1500ES (3/125)
$\lambda_{op}$ , nm	980	980	1310	1550	1550
$V$	2.2846	2.2702	2.2095	2.091	2.2632
$2a_{co}$ , $\mu\text{m}$	3.9505	5.0684	7.7074	7.3776	2.7900
$2a_{cor}$ , $\mu\text{m}$	4.0	5.1	7.7	7.4	2.8
$V_r$	2.3132	2.2844	2.2073	2.0973	2.2713
$MFD_r$ , $\mu\text{m}$	4.5159	5.8098	8.9981	9.0048	3.2030
$MFD$ , $\mu\text{m}^*$	4.5	5.8	9.0	9.0	3.2

\* From specification

The optical fiber parameters, as resulting from Tables 4 and 5, match accurately to the specifications of the manufacturer.

Fig. 6 presents a plot of refractive index of core ( $n_{co}$ ) and of cladding ( $n_{cl}$ ), for all five studied fibers, over all wavelength range (980 to 1650 nm). Notice that the curves of the refractive index of the core for SM980 (5.8/125) and SM1500 (9/125) superpose on the common wavelength range and they seem to belong to the same curve. This is explained (see Eq. (1)) by the fact that they have the same NA (0.14). As a matter of fact, there are only four different  $n_{co}$  curves because there are only four different values of NA (0.12, 0.14, 0.18 and 0.40).

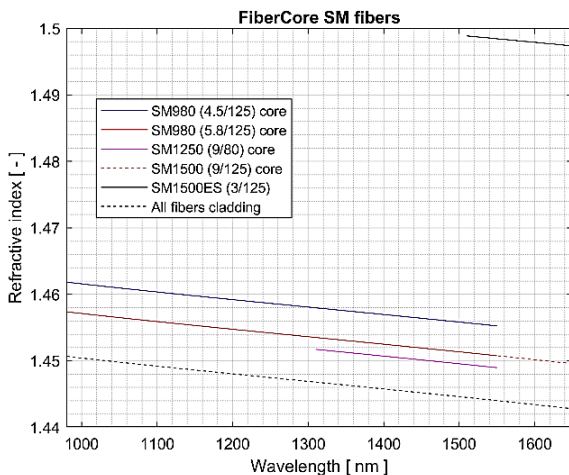


Fig. 6. Refractive index of core and cladding of some FiberCore single mode fibers (color online)

A plot of group refractive index of core ( $n_{gco}$ ) and of cladding ( $n_{gcl}$ ), for all five studied fibers, over all wavelength range (980 to 1650 nm) is shown in Fig. 7. The group refractive index is calculated as:

$$n_g = n - \lambda \cdot \frac{dn}{d\lambda} \quad (12)$$

resulting four different  $n_{gco}$  curves for the four values of NA.

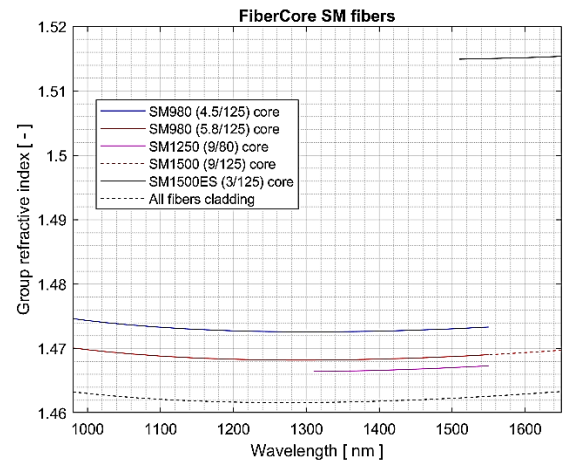


Fig. 7. Group refractive index of core and cladding of some FiberCore single mode fibers (color online)

The variation of  $V$  with wavelength (from 980 to 1650 nm) can be seen in Fig. 8. Notice that all  $V$  values are below 2.405 - that is the studied wavelength range is over the cut-off wavelength.

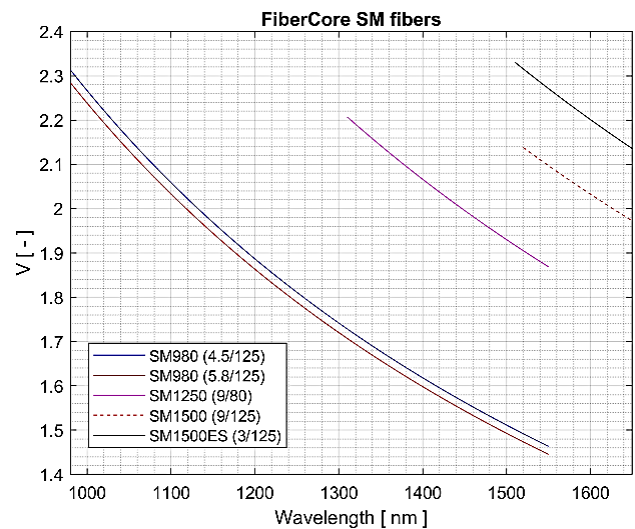


Fig. 8.  $V$  dependence on wavelength for some FiberCore single mode fibers (color online)

Fig. 9 illustrates the variation of  $MFD$  over the studied wavelength range.

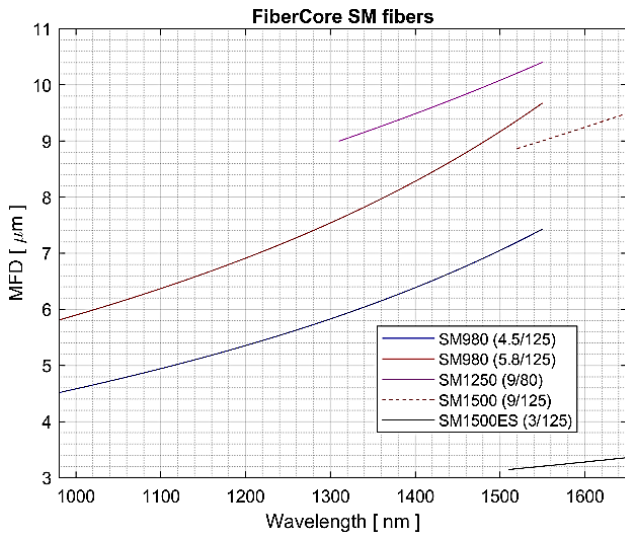


Fig. 9. MFD vs. wavelength for some FiberCore single mode fibers (color online)

#### 4. Discussion

The proposed procedure allows an accurate determination of  $NA$ ,  $MFD$  and  $a_{co}$ . The accuracy of determination was evaluated by calculating the relative difference between the calculated and the specified values of the parameters.

The accuracy of determination of  $NA$  (Table 6) was evaluated as very good since  $(NA-NA_{sp})/NA_{sp}$  lays between 0.05% and -0.42%, with an average of -0.10% and a standard deviation of 0.25%.

Table 6. Accuracy of determination of  $NA$

Optical fiber	$NA$	$NA_{sp}$	$(NA-NA_{sp})/NA_{sp}$
SM 980 (4.5/125)	0.1804	0.18	0.22%
SM 980 (5.8/125)	0.1397	0.14	-0.21%
SM 1250 (9/80)	0.1195	0.12	-0.42%
SM 1500 (9/125)	0.1398	0.14	-0.14%
SM 1500ES (3/125)	0.4002	0.40	0.05%

The accuracy of determination of  $MFD$  (Table 7) was evaluated as very good since  $(MFD-MFD_{sp})/MFD_{sp}$  lays between 0.05% and -0.51%, with an average of 0.07% and a standard deviation of 0.29%.

Table 7. Accuracy of determination of  $MFD$

Optical fiber	$MFD$	$MFD_{sp}$	$(MFD-MFD_{sp})/MFD_{sp}$
SMF 28e+ @1310nm	9.1535	9.2	-0.51%
SMF 28e+ @1550nm	10.4381	10.4	0.37%
SM 980 (4.5/125)	4.5159	4.5	0.35%
SM 980 (5.8/125)	5.8098	5.8	0.17%
SM 1250 (9/80)	8.9981	9	-0.02%
SM 1500 (9/125)	9.0048	9	0.05%
SM 1500ES (3/125)	3.2030	3.2	0.09%

The accuracy of determination of  $a_{co}$  couldn't be determined directly, because they weren't specified. Instead  $a_{co}$  determined  $MFD$ , which could be evaluated.

The accuracy of determination of the refractive index of core  $n_{co}$  was determined indirectly evaluating  $NA$  (see Eq. (1)).

#### 5. Conclusions

In this study a model of the optical fiber was elaborated to serve in Long Period Grating Fiber Sensors design. Starting from manufacturer specifications for mechanical and optical parameters all parameters needed in LPGFS design. All calculations were done as MATLAB functions, thus providing a useful toolkit for the designer.

The calculations were done in two variants according to the two approaches, depending on which parameters are specified by the manufacturer.

The tests made on several optical fibers of two major manufacturers proved a good concordance with given specifications.

Thus the model may be considered reliable and consistent.

#### Acknowledgments

This work was supported by the MANUNET grant MNET18/NMCS3474/98 and by the Core Program project no. PN 18 N/2019.

#### References

- [1] W. J. Bock, J. Chen, P. Mikulic, T. Eftimov, IEEE T. Instrum. Measur. **56**(4), 1176 (2007).
- [2] S. Miclos, D. Savastru, R. Savastru, F. G. Elfarra, I. Lancranjan, U.P.B. Sci. Bull. A **81**(3), 217 (2019).
- [3] K. T. Lau, C. C. Chan, L. M. Zhou, W. Jin, Compos. Part B Eng. **32**(1), 33 (2001).
- [4] D. Savastru, L. Baschir, S. Miclos, R. Savastru, I. I. Lancranjan, Compos. Struct. **245**, 112318 (2020).
- [5] I. Lancranjan, S. Miclos, D. Savastru, A. Popescu, J. Optoelectron. Adv. M. **12**(12), 2456 (2010).
- [6] P. Capoluongo, C. Ambrosino, S. Campopiano, A. Cutolo, M. Giordano, I. Bovio, L. Lecce, A. Cusano, Sensor Actuator. **133**(2), 415 (2007).
- [7] D. Savastru, S. Miclos, R. Savastru, F. G. Elfarra, I. Lancranjan, U.P.B. Sci. Bull. A **81**(2), 233 (2019).
- [8] R. Falciai, A. G. Mignani, A. Vannini, Sens. Actuators B Chem. **74**(1), 74 (2001).
- [9] S. Miclos, L. Baschir, D. Savastru, R. Savastru, I. I. Lancranjan, Compos. Struct. **256**, 113062 (2021).
- [10] D. Savastru, S. Miclos, R. Savastru, I. Lancranjan, J. Optoelectron. Adv. M. **20**(11-12), 610 (2018).
- [11] S. Miclos, D. Savastru, R. Savastru, F. G. Elfarra, I. Lancranjan, Optoelectron. Adv. Mat. **13**(1-2), 56 (2019).
- [12] A. D. Taylor, Q. Yu, S. Chen, J. Homola, S. Jiang, Sensor. Actuat. B-Chem. **107**(1), 202 (2005).

- [13] S. Balasubramanian, I. Sorokulova, V. Vodyanoy, A. Simonian, *Biosens. Bioelectron.* **22**(6), 948 (2007).
- [14] I. Abdulhalim, M. Zourob, A. Lakhtakia, *Electromagnetics* **28** (3), 214 (2008).
- [15] A. Popescu, S. Miclos, D. Savastru, R. Savastru, M. Ciobanu, M. Popescu, A. Lörinczi, F. Sava, A. Velea, F. Jipa, M. Zamfirescu, *J. Optoelectron. Adv. M.* **11**(11), 1874 (2009).
- [16] V. Nanduri, S. Balasubramanian, V. Vodyanoy, A. Simonian, S. Sista, *Anal. Chim. Acta* **589**(2), 166 (2007).
- [17] D. J. Monk, D. R. Walt, *Anal. Bioanal. Chem.* **379**(7-8), 931 (2004).
- [18] S. W. James, R. P. Tatam, *Meas. Sci. Technol.* **14**(5), R49 (2003).
- [19] T. Erdogan, *J. Opt. Soc. Am. A* **14**(8), 1760 (1997).
- [20] T. Erdogan, *J. Lightwave Technol.* **15**(8), 1277 (1997).
- [21] A. I. Kalachev, V. Pureur, D. N. Nikogosyan, *Opt. Commun.* **246**(1-3), 107 (2004).
- [22] C. S. Cheung, S. M. Topliss, S. W. James, R. P. Tatam, *J. Opt. Soc. Am. B* **25**(6), 897 (2008).
- [23] J. M. Lopez-Higuera, L. R. Cobo, *J. Lightwave Technol.* **29**(4), 587 (2011).
- [24] J. F. Akki, A. S. Lalasangi, P. U. Raika, T. Srinivas, L. S. Laxmeshwar, U. S. Raikar, *IOSR-JAP* **4**(3), 41 (2013).
- [25] Y. Koyamada, *IEEE Photonic. Tech. L.* **13**(4), 308 (2001).
- [26] D. Marcuse, *Bell Syst. Tech. J.* **56**, 703 (1977), doi:10.1002/j.1538-7305.1977.tb00534.x.
- [27] Refractive index database. Available online: <https://refractiveindex.info>. (accessed on 23 November 2020).
- [28] J. W. Fleming, *Appl. Opt.* **23** (24), 4486 (1984).

\*Corresponding author: miclos@inoe.ro